Applied Catalysis B: Environmental 111–112 (2012) 157–164

Contents lists available at SciVerse ScienceDirect

Applied Catalysis B: Environmental

journal homepage: www.elsevier.com/locate/apcatb

Deactivation characteristics of Ni/CeO_2-Al_2O_3 catalyst for cyclic regeneration in a portable steam reformer

Sungchul Lee[a,*], Gayatri Keskar[b], Changchang Liu[b], William R. Schwartz[b], Charles S. McEnally[b], Ju-Yong Kim[a], Lisa D. Pfefferle[b], Gary L. Haller[b]

[a] Energy Laboratory, Corporate R&D Center, Samsung SDI Co., Ltd, 428-5, Gongse-dong, Giheung-gu, Yongin-si, Gyeonggi-do 446-577, Republic of Korea
[b] Department of Chemical and Environmental Engineering, Yale University, P.O. Box 208286, New Haven, CT 06520, USA

ARTICLE INFO

Article history:
Received 3 August 2011
Received in revised form
10 September 2011
Accepted 25 September 2011
Available online 29 September 2011

Keywords:
Reformer
Nickel
Catalyst
Deactivation
Regeneration

ABSTRACT

The requirements of process parameters, e.g. air pump flow rate and operational pressure are restricted by confined space and limit the performance of portable steam propane reformer. This makes it difficult to operate a catalyst in the portable reformer under mild operation conditions. Hence, the catalyst can be rapidly deactivated. The deactivation behavior of Ni/CeO_2-Al_2O_3 catalyst was investigated for coke deposition and active metal sintering. Coke formation by the propane pyrolysis was predominantly responsible for deactivation at low reaction temperature. Coke formation can be thermodynamically reduced by elevating the temperature and hence the steam reformer was operated at high temperature to inhibit coke formation. Although the Ni/CeO_2-Al_2O_3 catalyst made small amounts of coke at high temperature, it was deactivated by the encapsulated carbon on active metal during long term operation. Because a compact air pump for catalyst regeneration was available during the shut-down procedure of our portable fuel cell system, the catalysts could be regenerated by coke oxidation. The cyclic oxidation was useful for long term operation. The properties of the used catalyst and the coke were investigated by XRD, NEXAFS, XANES-TPO, TGA and TEM. The Ni/CeO_2-Al_2O_3 catalyst in our portable reformer showed stable activity for steam propane reforming in cyclic oxidation operation for 500 h.

1. Introduction

Polymer electrolyte fuel cell (PEFC) systems are good candidates to commercialize because of their various applications, such as a portable power system for outdoor activity and off-grid power supply system. These applications require fuel accessibility, high energy density of fuel and robust system control. Hydrocarbon-based fuels, such as liquefied petroleum gas (LPG), gasoline, diesel, and alcohol can be used as fuel sources for a portable fuel cell system [1–5]. Commercial propane is readily available (at any gas station or supermarket in the Republic of Korea) and is widely used for outdoor applications. Because LPG can be easily vaporized at room temperature, the fuel feeding of LPG is effective and easily controlled in a fuel cell system.

The portable steam reformer requires the availability of various components: (1) the flow rates and operational pressure of the air pump are restricted due to the limited available space and electric power for the compact system, (2) the steam reformers used for this application should have a wide operating range compared to industrial plants, making it easier to select the optimal operating parameters, (3) the catalysts may be regenerated without additional equipment, e.g., switching regenerator, (4) the reformer requires some electric power, which comes from the integrated battery in the system, to start, shut down and regenerate the catalysts and it is important to minimize additional power consumption of the integrated battery, and (5) although mild regeneration procedures improve the stability against to catalyst sintering, air oxidation is a reasonable technique for the regeneration of catalysts in the portable fuel cell system.

Nickel based catalysts, i.e. Ni/Al_2O_3, Ni/CeO_2-Al_2O_3 and Ni-Mg/Al_2O_3 are remarkably active for steam reforming of light hydrocarbons at low temperature [6–11]. However, coke formation and the active metal sintering are expected to cause deactivation of Ni catalysts. The methods of preventing catalytic deactivation by coke deposition are coke minimization control and regeneration of deactivated catalyst. The first approach is coke minimization that controls the number of active sites in an ensemble and prevents the formation of metal carbide by the addition of secondary metals [12–16]. The second approach to prevent catalytic deactivation by coke build up is regenerative removal of the coke formed on the catalytic surface during steam reforming. Typically in industry, O_2 or air is used to oxidize coke in the regenerator [17]. During the regeneration step, a hot spot may form in the catalyst bed, and a part of the catalyst may be sintered. To minimize catalyst

* Corresponding author. Tel.: +82 31 288 4878.
E-mail addresses: scat.lee@samsung.com, sc673.lee@gmail.com (S. Lee).

0926-3373/$ – see front matter © 2011 Elsevier B.V. All rights reserved.
doi:10.1016/j.apcatb.2011.09.030

sintering, coke removal by different gasifying agents, such as O_2, air, CO_2, H_2 and N_2, have been studied [18]. The performance of the gasifying agents decreases in the order O_2 > air > CO_2 > H_2 > N_2. This literature, which suggested that the efficient coupling of air oxidation ($C_{(s)} + O_{2(g)} \rightarrow CO_{2(g)}$, $\Delta H^\circ = -394.5$ kJ/mol) and reverse Boudouard reaction ($C_{(s)} + CO_{2(g)} \rightarrow 2CO_{(g)}$, $\Delta H^\circ = 175.2$ kJ/mol), led to better regenerative operation for reducing catalyst sintering. During start-up and shut-down operation of the residential fuel cell system, the catalyst beds are purged by steam for safety reasons [19]. Steam feeding without any fuel can deactivate the Ni based catalyst, because the steam quickly oxidizes the Ni metal. Li et al. have reported improvement in the thermal stability of Ni/Mg(Al)O catalyst by the addition of small amounts of precious metals. The metallic Ni particles are re-dispersed on the catalyst surface, resulting in high and stable activity [20].

Comparing Ni/CeO_2-Al_2O_3 catalysts with Ni/Al_2O_3 catalysts used for steam reforming, we know that Ni/CeO_2-Al_2O_3 catalyst exhibits OSC, a function necessary for oxidation of surface carbons and hydrocarbons. In this study, steam reforming reactions of Ni/CeO_2-Al_2O_3 catalyst were carried out at different reaction temperatures (500, 600, 700 and 800 °C). After reaction for 5 h, the Ni metal particle size and amount of coke were measured using various characterization methods. The Ni metal particle sizes after oxidation were measured to study the stability of regeneration (where reaction and regeneration temperatures were the same). Finally, we investigated both steady-state operation and cyclic oxidation operation of Ni/CeO_2-Al_2O_3 catalyst for 500 h. The relationship between the high temperature stability and the properties of Ni/CeO_2-Al_2O_3 catalyst were studied during the steam reforming reaction.

2. Experimental

2.1. Preparation of catalysts

Two kinds of catalysts, powder and monolith samples, were prepared. The CeO_2-Al_2O_3 support with a nominal Al/Ce molar ratio of 13.5 was prepared by physically mixing gamma aluminum oxide (γ-Al_2O_3, Alfa Aesar) and cerium oxide (CeO_2, Aldrich) in water. Ni/CeO_2-Al_2O_3 catalyst was prepared by impregnation (Ni/Ce/Al molar ratio = 0.08/0.06/0.86, surface area = 120.7 m^2/g, and pore volume = 0.34 cm^3/g). Nickel (II) nitrate hexahydrate ($Ni(NO_3)_2 \cdot 6H_2O$, Aldrich) was used as the metal source. The Ni solution was prepared by dissolving nickel(II) nitrate hexahydrate in 150 ml of water and the CeO_2-Al_2O_3 support was suspended in 100 ml of water. Each solution was stirred for 1 h. The Ni solution was added to the suspended CeO_2-Al_2O_3 solution, and then the final mixture was refluxed at the boiling temperature for 40 h. After refluxing, the sample was evaporated and dried at 100 °C in a vacuum oven. For the monolith catalyst, the refluxed slurry was coated on cordierite (600 cpsi) and dried at 100 °C in a vacuum oven. The dried samples were finely ground and calcined under flowing air at 540 °C for 6 h.

2.2. Characterization

The properties of the Ni/CeO_2-Al_2O_3 catalyst were characterized by X-ray diffraction (XRD, Bruker, AXS D8Focus diffractometer), and transmission electron microscopy (TEM, TECNAI TF20 FEG TEM/STEM). To determine the Ni oxidation state and local atomic structures, in situ and ex-situ X-ray absorption measurements were performed at the Ni K edge (8333 eV) using the Si (1 1 1) monochromator crystal at X18B beamline at the National Synchrotron Light Source, Brookhaven National Laboratory. One hundred mg of each sample were pressed into a self-supporting wafer and placed in a stainless steel cell equipped with beryllium (0.5 mm thick, Aldrich) windows, gas inlet and outlet, liquid nitrogen cooling line, and heating elements allowing the in situ controlled atmosphere treatments up to 750 °C. To investigate the effect of oxidation temperature, each sample was oxidized at 750 °C by flowing 10% O_2/He for 30 min to 1 h and quenched to room temperature using liquid nitrogen. X-ray absorption near edge structure (XANES) spectra were collected during sample oxidation with a 5 min interval between the scans [21–23].

A temperature programmed oxidation (TPO) technique was used to characterize the oxidized samples by mass spectrometry. Approximately 50 mg of each sample was loaded into a quartz cell. Prior to each TPO run, the sample cell was purged by ultra zero grade air at room temperature, and the baseline was monitored until stable. After baseline stabilization, the sample cell was heated at a rate of 10 °C/min and held for 1 h at 800 °C to ensure complete metal and coke oxidation.

Thermal gravimetric analysis (TGA) was used to determine the amount of coke formed. TGA data were collected in a Setaram Setsys 1750 instrument under air flow. Samples were heated to 150 °C in pure argon for 1 h to dehydrate before initiating the temperature program. The initial weight change of the sample was measured between 150 and 1000 °C, when heated at 10 °C/min for two successive ramps. The second ramp was used as a baseline correction for the first.

2.3. Steam reforming reaction

Propane steam reforming reaction was carried out in a fixed bed reactor (16 mm-ID × 600 mm-high). The powder catalyst (500 mg) was loaded for the catalytic activity study, and the monolith sample (16 mm-OD × 100 mm-high) was loaded the long term activity studies. The flow rates of reactants (C_3H_8 and air) and internal standard (N_2) gases were controlled by using a mass flow controller (MFC). A syringe pump was used to feed water in to the system. The powder and the monolith catalysts operated at a space velocity of 36000 ml/g-cat h and 7200 h^{-1} respectively. Gas compositions were measured by a real-time gas analyzer after removing the water from the reformate gas. The real-time gas analyzer (Rosemount) was equipped with a non-dispersive infrared detector for CO, CO_2 and CH_4 and a thermal conductivity detector for H_2. The flow rate of the dried reformate gas was measured by wet gas meter (Shinagawa). For reaction-oxidation cycles, every cycle was composed of a propane steam reforming for 10 h and an air oxidation (air flow rate = 400 ml/min) at the same reaction temperature for 10 min.

3. Results and discussion

3.1. Characterization of Ni/CeO_2-Al_2O_3 catalyst after propane steam reforming

Nickel supported on CeO_2-Al_2O_3 catalysts were evaluated for propane steam reforming. Cerium oxide exhibits the OSC function, which can oxidize surface carbon and propane. For Ni/Al_2O_3 catalyst, the formation of carbon filaments caused Ni particles to detach from the support thus leading to catalytic deactivation. However, we believe that Ni particles on CeO_2 promoted catalyst remained on the Al_2O_3 support due to the strong interaction of Ni with the support. The activity of Ni/CeO_2-Al_2O_3 catalyst was studied by temperature programmed reaction (heating rate = 5 °C/min) with a constant steam/carbon ratio (S/C = 3), propane flow rate (30 ml/min) and reaction pressure (1 atm). Fig. 1 reveals the results of temperature programmed propane steam reforming on the Ni/CeO_2-Al_2O_3 catalyst. The H_2 and CO concentrations gradually

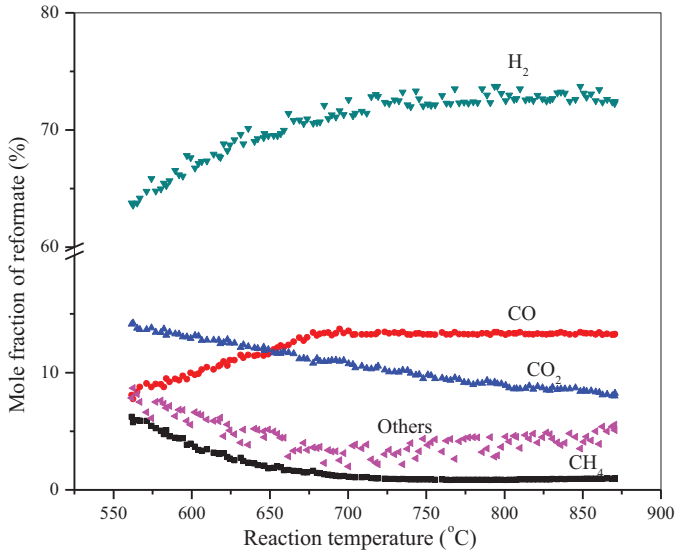

Fig. 1. The result of temperature programmed propane steam reforming on Ni/CeO_2-Al_2O_3 catalyst.

increased as the reaction temperature approached 700 °C. The maximum H_2 and CO concentrations were 72.9% and 13.3% each. Further increase in the temperature led to an unchanged composition. These results are consistent with the results of thermodynamic calculation by Wang et al. [24]. Increasing CO concentration at high temperature was attributed to the exothermic water gas shift reaction and the endothermic steam reforming reaction. The CH_4 in the propane steam reforming was produced through CO_2 or CO methanation. One mole of CH_4 was produced at the cost of 3 or 4 moles of H_2. Therefore the CH_4 concentration in the reformate gas should be minimized for high reforming efficiency [25,26]. Because methanation is not favored at high temperature, the operating temperature of Ni/CeO_2-Al_2O_3 catalyst must be above 700 °C to maximize the efficiency of the reformer. Although the steam reforming activity and selectivity were enhanced at high temperature, we propose that the Ni/CeO_2-Al_2O_3 catalyst at high temperature may have deactivated due to the sintering of active metal.

Fig. 2 shows the TEM images of Ni/CeO_2-Al_2O_3 catalysts after being reacted at different reaction temperatures. The particle size of the fresh Ni/CeO_2-Al_2O_3 catalyst varied from 7 to 15 nm (Fig. 2(a)). As shown in Fig. 2(b), numerous carbon filaments or tubes were observed on the catalyst surface. While most of the carbon at 500 °C was in the form of carbon filaments, carbon nanotubes (CNT) were generated at 700 °C. There were significantly larger particles on the catalyst surface after reaction at 800 °C. The diameters of carbon fibers formed by the thermal pyrolysis of propane at 500 °C varied from 20 nm to 50 nm. Hermann et al. reported that CNT growth was affected by the temperature, pressure and gas compositions [27]. In particular, the reaction temperature determines the diameter of CNT. It is estimated that the porosity of the used catalysts might have changed by the CNT formed during the reaction (See Supplemantry Fig. S1). The amounts of carbon deposition on the

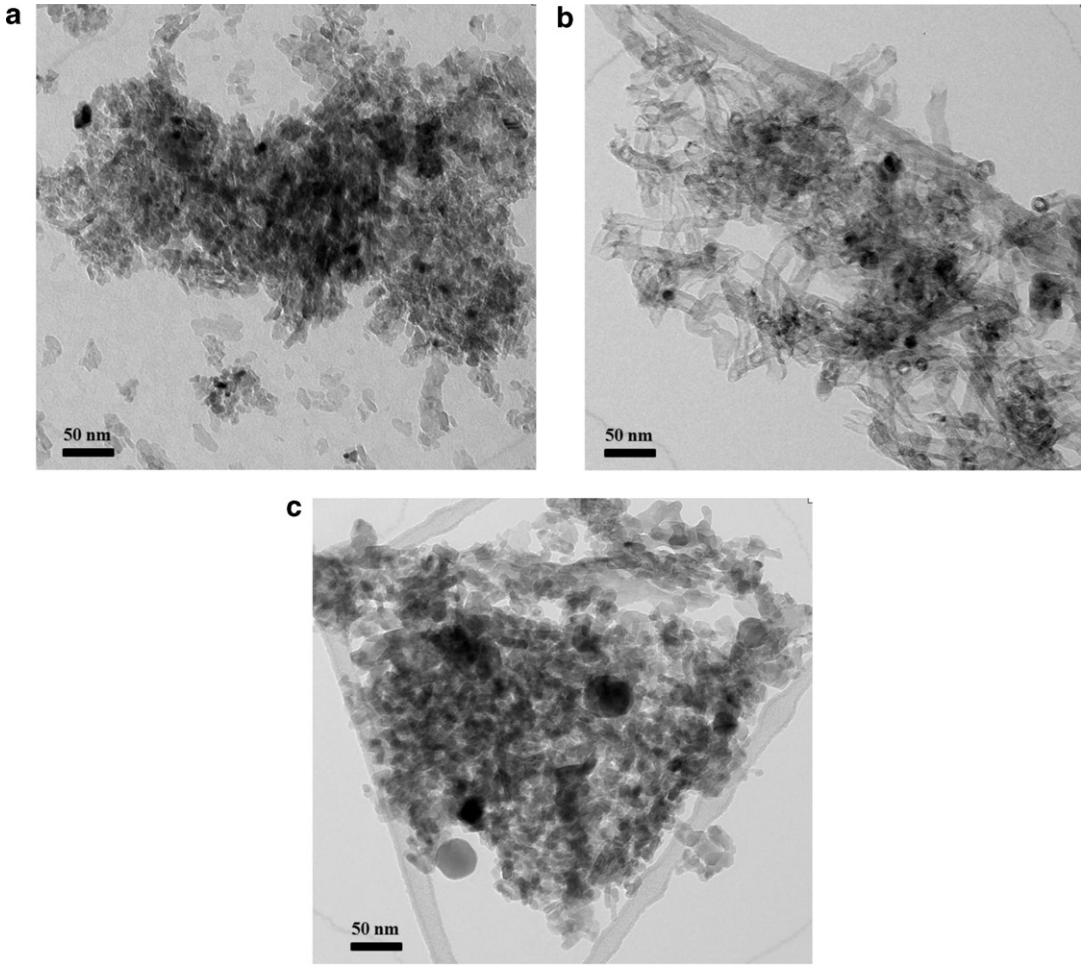

Fig. 2. TEM images of Ni/CeO_2-Al_2O_3 catalysts after being reacted at different reaction temperatures: (a) fresh; (b) 700 °C; (c) 800 °C.

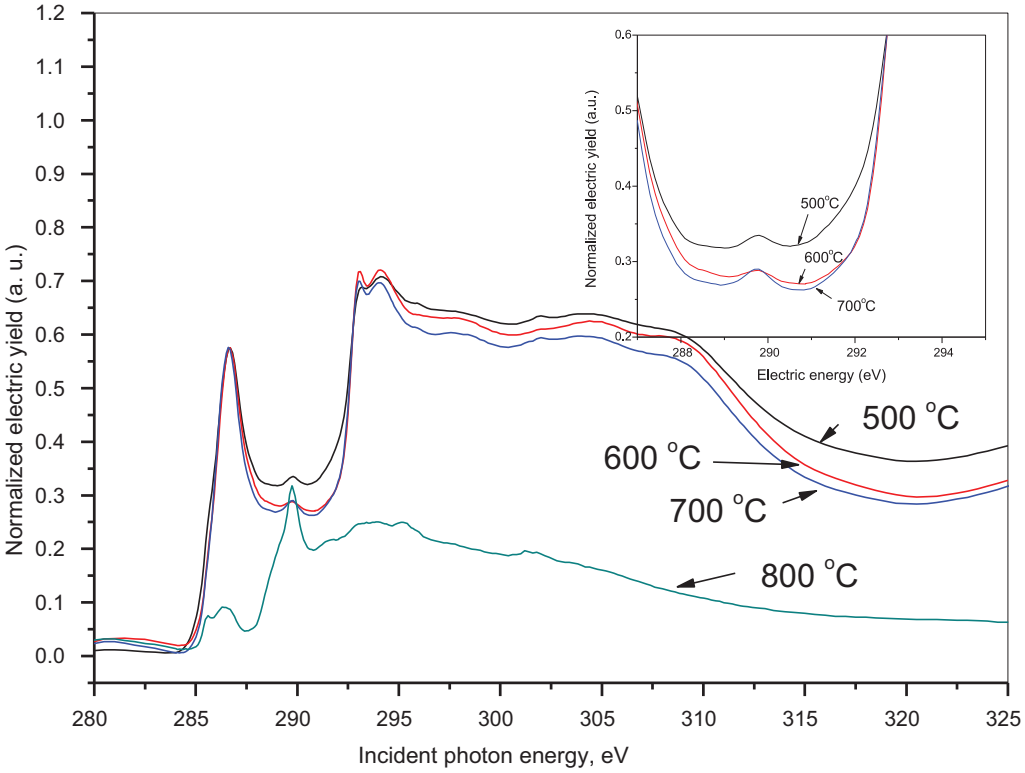

Fig. 3. Carbon k-edge NXANES spectra of Ni/CeO_2-Al_2O_3 catalysts after being reacted at different reaction temperatures. The spectra of 500, 600 and 700 °C reacted catalyst have similar shape and are normalized at the π* aromatic structure resonance maximum. The shape of the 800 °C reacted catalyst is very different (does not have any aromatic carbon/coke) and is not rescaled.

Ni/CeO_2-Al_2O_3 catalyst were measured by TGA (Table 1). Carbon deposition is an important component of the deactivation of the Ni based catalyst. Coke deposition has a strong dependence on the nature of Ni particles. Carbidic carbon can be a precursor graphitic carbon that causes deactivation [28,29]. Thermodynamically, coke formation can be inhibited above 750 °C with a steam to carbon (S/C) ratio greater than 2 regardless of the temperature [24]. However, the Ni/CeO_2-Al_2O_3 catalyst was deactivated, in spite use of S/C = 3, due to carbon deposition. During propane steam reforming, 1.5 g/h-cat g of carbon was deposited on the Ni/CeO_2-Al_2O_3 catalyst, at 500 °C, whereas the amount of carbon deposition was drastically reduced at 800 °C. The amount of carbon deposition was decreased by increasing reaction temperature.

The C k-edge of near edge X-ray absorption fine structure (NEXAFS) spectra provides structural information about atoms, molecules, and local chemical functionalities. The sharp peak at about 285 eV is assigned to the transitions of the π* resonance of the aromatic structure, and the broad peak above 290 eV is C–C σ* resonance [30]. The region between 287 and 290 eV corresponds to the C–O bonding, with 287.6 eV assigned to C–O π* resonance and 288.2 eV assigned to the C–O σ* transition [31,32]. The coked catalyst also has the characteristic C k-edge features of transition metal carbides at 286.7 and 289.5 eV [33,34]. Fig. 3 shows the C k-edge NEXAFS spectra for used catalysts with different reaction temperatures. The C k-edge spectrum measured at 25 °C showed peaks at 286.7, 289.8, 293.2, 294.1, 296.0, 297.4, 302.0, and 304.8 eV (not shown). A close similarity in the C k-edge of the NEXAFS for used catalysts at 500, 600 and 700 °C was observed, but the intensity of C k-edge NEXAFS of the samples reacted at 800 °C was very low relative to that of the samples at 500, 600 and 700 °C. The main peak of the spectrum for the sample at 800 °C was observed at 289.7 eV, along with the small peaks at 286.7 and 293.2 eV. It is suggested that the pathway of coke formation at high temperature is quite different from that at lower temperature. The Ni active sites favored the formation of the carbidic carbon at high temperature (evidenced by the high intensity at 289.7 eV), which was a precursor of graphitic carbon. The graphitic carbon encapsulated the active sites on the surface, which subsequently caused the deactivation.

XRD patterns of the Ni/CeO_2-Al_2O_3 catalyst after steam reforming at different reaction temperatures are presented in Fig. 4. After steam reforming, the peak corresponding to γ-Al_2O_3 phase disappeared and the peak intensity of CeO_2 significantly increased with increasing reaction temperature. This was due to the formation of CeO_2 which covered the γ-Al_2O_3 phase, and certain peaks of the CeO_2 phase overlapped with that of γ-Al_2O_3 phase. For Ni/CeO_2-Al_2O_3 catalyst after reaction at 800 °C, the peak at $2\theta = 33.3°$ was

Table 1
Total coke contents before and after regeneration.

Reaction and regeneration temperature (°C)	Amount of carbon deposit (g/h-cat g)	Total remained coke after regeneration (g/h-cat g)	Total coke removed after regeneration (%)
500	1.541	0.706	54.2
600	0.485	0.004	99.1
700	0.493	0	100
800	0.123	0	100

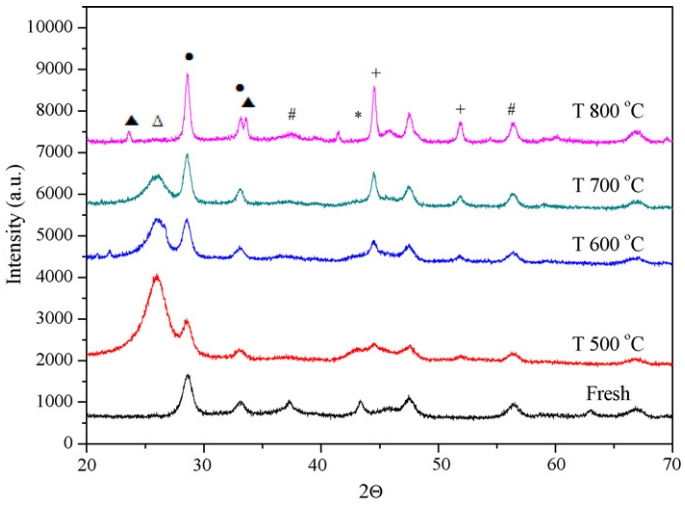

Fig. 4. X-ray diffraction patterns of Ni/CeO_2-Al_2O_3 catalysts after propane steam reforming at different reaction temperatures. (+) Ni, (*) NiO, (#) Al_2O_3, (●) CeO_2, (▲) $CeAlO_3$, (△) Graphite.

detected which indicated that a portion of CeO_2 interacted with the Al_2O_3 [15,35]. Shyu et al. [35] reported that a small CeO_2 crystallite on Al_2O_3 could be transformed to $CeAlO_3$ at reduction temperature above 600 °C, while even a partial conversion to $CeAlO_3$ from the large CeO_2 particles required a temperature above 800 °C. The formation of $CeAlO_3$ was helpful for the thermal stability under oxidation conditions [35,36]. The XRD peak corresponding to graphitic carbon at $2\theta = 26.4°$ was observed for the used catalysts (at 500, 600 and 700 °C). The peak intensity of graphite was the highest at 500 °C, and then it decreased with the increased reaction temperature. The peak corresponding to graphite was not observed in the reaction sample at 800 °C. This result is consistent with the TEM results (presented in Fig. 2) and the C k-edge NXANES (see Fig. 3) exhibiting a strong π^* aromatic C resonance at 500, 600 and 700 °C which disappears at 800 °C reaction temperature. The NiO ($2\theta = 43.4°$) used for fresh Ni/CeO_2-Al_2O_3 catalyst was reduced during the propane steam reforming reaction. The peak of NiO disappeared with increasing reaction temperature, and then that of metallic Ni at $2\theta = 44.4°$ emerged concomitantly. The peak of metallic Ni became sharper and narrower with increased reaction temperature. The particle sizes of the CeO_2, NiO and metallic Ni were calculated by the X-ray line broadening Scherrer equation analysis (Table 2). The particles of the CeO_2 and metallic Ni were sintered at high temperature.

Table 2
Particle size of metal oxide before and after reaction with different temperatures.

Reaction temperature (°C)	Particle size (nm)		
	CeO_2 ($2\theta = 28.4$)	NiO ($2\theta = 43.3$)	Ni ($2\theta = 44.5$)
Fresh	9.2	10.1	–
500	7.1	7.2	4.7
600	10.4	–	11.4
700	12.1	–	16.3
800	18.4	–	21.8

The first-row transition metal elements exhibited well-defined site symmetry spectra in the XANES analysis. Normalized Ni k-edge XANES spectra of Ni/CeO_2-Al_2O_3 catalysts after steam reforming at different temperature are shown in Fig. 5. The standard edge energy was calibrated at the first inflection point in the foil calibration spectrum (8333.0 eV), which measured the threshold of photoejection of the 1s electron (k-edge) in nickel metal [37–39]. The pre-edge peak intensity and white line intensity are considered the main features reflecting the oxidation state of Ni on the CeO_2-Al_2O_3 support. The intensity of the white line decreased and that of pre-edge increased with increasing reaction temperature. NiO on the surface of CeO_2-Al_2O_3 was almost reduced to Ni metal causing it to agglomerate on the surface and therefore, the Ni-XANES spectrum of the reacted sample at 800 °C was similar to that of the Ni-foil. This result indicated that the lattice Ni was reduced to form metallic Ni particles. For better comparison, the derivative spectra of all samples are presented in Fig. 5(b). The derivate spectrum of the used catalyst at 500 °C was similar to that of NiO reference, and the spectra of the rest of the samples were evaluated as the sum of Ni metal and contributions from the $NiAl_2O_4$. The low temperature (500 °C) operation of steam reforming was insufficient to reduce NiO to Ni, which formed the active sites. The Ni/CeO_2-Al_2O_3 catalyst was reduced in the reforming reaction above 600 °C without additional pre-reduction treatment.

The properties of Ni/CeO_2-Al_2O_3 catalyst after reaction at different temperatures were measured by XRD, XANES, TEM and TGA. When this catalyst was operated at high temperature, coke formation was inhibited. After the reaction of Ni/CeO_2-Al_2O_3 catalyst at 800 °C, an interaction between the CeO_2 and Al_2O_3 was observed

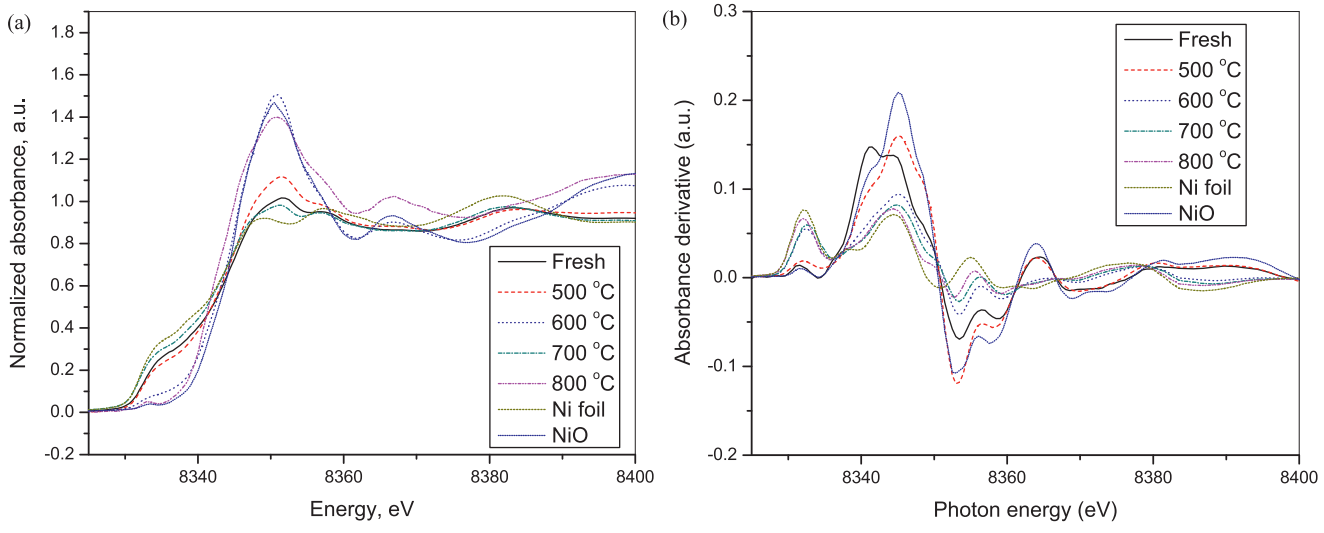

Fig. 5. XANES spectra of Ni/CeO_2-Al_2O_3 catalysts after being reacted at different reaction temperatures: (a) normalized XANES spectra; (b) derived XANES spectra.

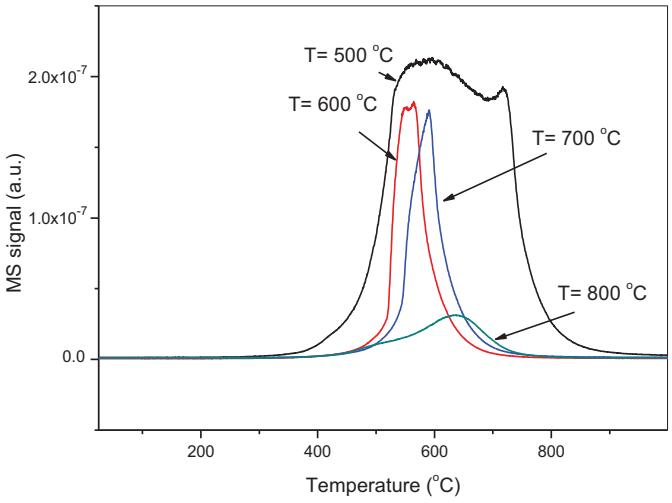

Fig. 6. Temperature programmed oxidation for Ni/CeO_2-Al_2O_3 catalysts after propane steam reforming for 5 h at different reaction temperatures.

3.2. Regeneration of Ni/CeO_2-Al_2O_3 catalyst after propane steam reforming

The TPO patterns are presented for Ni/CeO_2-Al_2O_3 catalysts after the propane steam reforming reaction for 5 h at different reaction temperatures in Fig. 6. Amorphous carbon, which was formed on the Ni/CeO_2-Al_2O_3 surface randomly during the reaction at 500 °C, was oxidized over a wide temperature range (400–800 °C). The Ni phase peak for the rest of the samples shifted to the higher temperature with increasing reaction temperature. We propose that the thin CH_x film or few layers of graphite encapsulate the active sites on the surface making the coke located at the surface of Ni particles difficult to oxidize [40].

The regeneration time and temperature of this reforming system are limited due to its application as a portable fuel cell system. In particular, the maximum temperature during the regeneration procedure should not be above the operation temperature. The coke oxidation behaviors at the reaction and regeneration temperatures are presented in Supplementary Fig. S2. We can estimate the amount of the coke, which is oxidized at the operation temperature in two oxidation steps. First, air was injected for 60 min after reaction temperature was attained. The carbon remaining after the first regeneration step was completely oxidized at 800 °C. The cokes formed at 500 and 600 °C were not completely removed at the regeneration temperature up to 1 h. The total carbon analysis after regeneration is presented in Table 1. At 500 °C, 54% of the total coke was oxidized and the total carbon from the regenerated catalyst was 0.706 g/h-cat g. The coke was completely removed above 700 °C in the second step. Therefore, the reaction and regeneration temperatures should be operated above 600 °C.

To investigate the thermal stability of Ni particles during the regeneration, in situ XANES of coked catalysts was conducted. The in situ XANES-TPO was performed using ultra zero grade air from room temperature to 750 °C at 20 °C/min and continuously monitoring the state of Ni in the coked catalyst at 750 °C for 30 min, as shown in Fig. 7 and Supplementary Fig. S3. The pre-edge peak and white line intensity were considered as the main features to examine the oxidation of Ni. For the used catalyst more dramatic changes were observed for the Ni k-edge XANES at higher temperatures (600–800 °C). Both the edge shift and an increase in the white line intensity were observed for the after reaction catalysts at 600, 700, 800 °C when heated in air, whereas the after reaction catalyst at 500 °C remained largely unchanged during the regeneration procedure. These observed changes for high temperature reaction samples can be attributed to the oxidation of Ni from the metallic Ni to Ni^{2+} species during the regeneration procedure.

The catalytic activities of the steady state operation and the reaction-oxidation cycles were compared at 800 °C for 500 h to study the thermal stability of Ni/CeO_2-Al_2O_3 catalyst during the reaction-oxidation cycle. The profiles of H_2 yield and CH_4 selectivity during the reaction-oxidation cycles and the steady state operation are displayed in Fig. 8. The H_2 yield of Ni/CeO_2-Al_2O_3 catalyst under steady state operation remained unchanged for 200 h, whereas the CH_4 concentration was gradually increased, as shown in Fig. 8(a). Furthermore, the H_2 yield started to drop after 200 h and finally reached 91% after 500 h. The deposited coke was partially removed by the released H_2, and hence the CH_4 concentration increased gradually due to the methanation of deposited coke. Despite of the high temperature operation for coke minimization, these results indicate that the Ni/CeO_2-Al_2O_3 catalyst was deactivated due to accumulation of coke. For reaction-oxidation cycles, every cycle was composed of a propane steam reforming for 10 h and an air oxidation for 10 min. This cyclic oxidation completely oxidized the

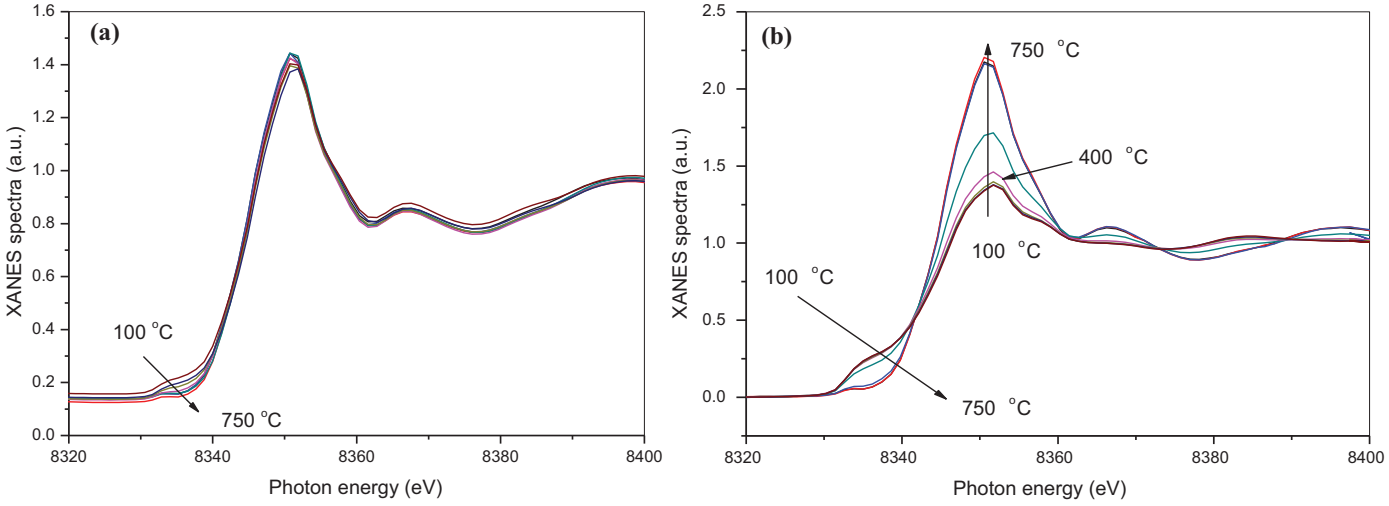

Fig. 7. In-situ Ni k-edge XANES TPO results of Ni/CeO_2-Al_2O_3 catalysts after propane steam reforming at different reaction temperatures: (a) 500 °C; (b) 600 °C.

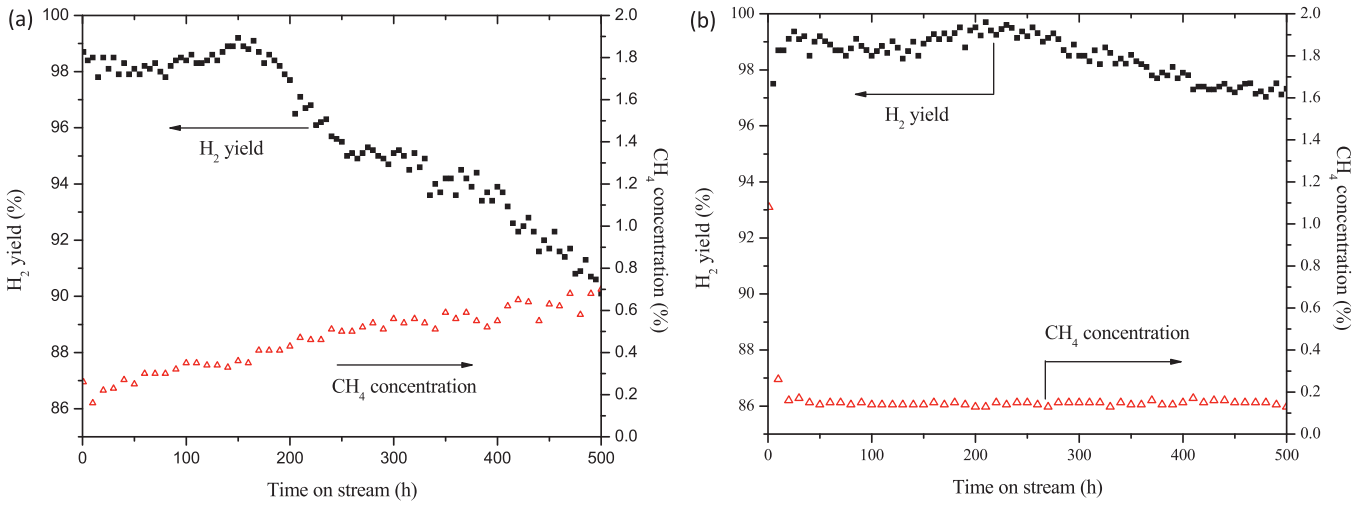

Fig. 8. Hydrogen yield and CH_4 selectivity during (a) the steady state operation and (b) the reaction-oxidation cycles (10 h of propane reforming followed by 10 min air oxidation regeneration).

coke formed during the steam reforming step to prevent an accumulation of coke on the catalyst (see Supplementary Fig. S2). The Ni/CeO_2-Al_2O_3 catalyst was used under both conditions without a pre-reduction step because of the in situ reduction by the produced H_2. The H_2 yield in the steady state operation was 98% for about 200 h, and afterwards the catalytic activity decreased rapidly. After the steady state condition for 500 h, the H_2 yield was decreased to 89%. However the H_2 yield of Ni/CeO_2-Al_2O_3 catalyst in the cyclic oxidation operation was 99% up to 500 h, which is close to the theoretical value. The complete (average) H_2 yield was steady for about 250 h, and then decreased continuously after the 24th cycle (~250 h). The H_2 yield for the 49th cycle (~500 h) was 96%. Although the coke formation was inhibited at 800 °C, the catalyst was deactivated rapidly without the coke oxidation treatment.

4. Conclusion

The properties of Ni/CeO_2-Al_2O_3 catalyst after reaction at different reaction temperatures were measured. The use of this catalyst at high temperature inhibited coke formation. However, the coke formation pathway at high temperature was different. The Ni active sites favored the formation of the carbidic carbon at high temperature, which acted as a precursor for graphitic carbon. The graphitic carbon encapsulated the active sites on the surface, which resulted in deactivation of the catalyst. After the reaction of Ni/CeO_2-Al_2O_3 catalyst at 800 °C, an interaction between CeO_2 and Al_2O_3 was detected.

The reforming system in the portable fuel cell system has limitations on the regeneration time and temperature. Therefore, it is important to regenerate the deactivated catalyst by simple methods. Although Ni/CeO_2-Al_2O_3 catalyst had small amount of coke, after reaction at high temperature, it was deactivated during the long term propane steam reforming for 500 h. Cyclic oxidation was beneficial for the long term test for which the H_2 yield of the 49th cycle was 96%. The deactivation rate under the cyclic oxidation condition is lower than that under the steady state condition at high temperature in the long term test.

Acknowledgements

We acknowledge National Synchrotron Light Source at Brookhaven National Laboratory for X-ray beamtime at beamline X18B and UV beam time at U4B.

Appendix A. Supplementary data

Supplementary data associated with this article can be found, in the online version, at doi:10.1016/j.apcatb.2011.09.030.

References

[1] M. Nilsson, X. Karatzas, B. Lindström, L.J. Pettersson, Chem. Eng. J. 142 (2008) 309–317.
[2] B. Lindström, J.A.J. Karlsson, P. Ekdunge, L.D. Verdier, B. Häggendal, J. Dawody, M. Nilsson, L.J. Pettersson, Int. J. Hydrogen Energy 34 (2009) 3367–3381.
[3] J. Mathiak, A. Heinzel, J. Roes, T. Kalk, H. Kraus, H. Brandt, J. Power Sources 131 (2004) 112–119.
[4] A. Ersöz, Int. J. Hydrogen Energy 33 (2008) 7084–7094.
[5] S. Lee, W.R. Schwartz, J. Choi, J. Ahn, D. Kim, I. Son, W. Shin, J. Kim, Int. J. Hydrogen Energy 35 (2010) 12286–12294.
[6] J. Seo, M. Youn, S. Park, J. Jung, P. Kim, J. Chung, I. Song, J. Power Sources 186 (2009) 178–184.
[7] Y. Li, X. Wang, C. Xie, C. Song, Appl. Catal. A-Gen. 357 (2009) 213–222.
[8] J.J. Strohm, J. Zheng, C. Song, J. Catal. 238 (2006) 309–320.
[9] S. Andonova, C.N. de Ávila, K. Arishtirova, J.M.C. Bueno, S. Damyanova, Appl. Catal. B-Environ. 105 (2011) 346–360.
[10] L. Zhang, W. Wang, B. Tan, U.S. Ozkan, J. Mol. Catal. A-Chem. 297 (2009) 26–34.
[11] M. Watanabe, H. Yamashita, X. Chen, J. Yamanaka, M. Kotobuki, H. Suzuki, H. Uchida, Appl. Catal. B-Environ. 71 (2007) 237–245.
[12] D.L. Trimm, Catal. Today 49 (1999) 3–10.
[13] A.S.A. Al-Fatish, A.A. Ibrahim, A.H. Fakeeha, M.A. Soliman, M.R.H. Siddiqui, A.E. Abasaeed, Appl. Catal. A-Gen. 364 (2009) 150–155.
[14] Z. Zhang, X.E. Verykios, S.M. MacDonald, S. Affrossman, J. Phys. Chem. 100 (1996) 744–754.
[15] N. Srisiriwat, S. Therdthianwong, A. Therdthianwong, Int. J. Hydrogen Energy 34 (2009) 2224–2234.
[16] S. Corthals, J.V. Nederkassel, J. Geboers, M.D. Winne, J.V. Noyen, B. Moens, B. Sels, P. Jacobs, Catal. Today 138 (2008) 28–32.
[17] A.S.A. Al-Fatesh, A.A. Ibrahim, A.H. Fakeeha, A.E. Abasaeed, M.R.H. Siddiqui, J. Ind. Eng. Chem. 17 (2011) 479–483.
[18] F. Alenazey, C.G. Cooper, C.B. Dave, S.S.E.H. Elnashaie, A.A. Susu, A.A. Adesina, Catal. Commun. 10 (2009) 406–411.
[19] D. Li, T. Shishido, Y. Oumi, T. Sano, K. Takehira, Appl.Catal. A-Gen. 332 (2007) 98–109.
[20] D. Li, Y. Zhang, K. Nishida, Y. Oumi, T. Sano, T. Shishido, K. Takehira, Appl. Catal. A-Gen. 363 (2009) 169–179.
[21] S. Lee, C.Z. Loebick, L.D. Pfefferle, G.L. Haller, J. Phys. Chem. C 115 (2011) 1014–1024.
[22] C.Z. Loebick, S. Lee, S. Derrouiche, M. Schwab, Y. Chen, G.L. Haller, L.D. Pfefferle, J. Catal. 271 (2010) 358–369.
[23] N. Li, X. Wang, S. Derrouiche, G.L. Haller, L.D. Pfefferle, ACS Nano 4 (2010) 1759–1767.
[24] X. Wang, N. Wang, J. Zhao, L. Wang, Int. J. Hydrogen Energy 35 (2010) 12800–12807.
[25] S. Wang, S. Wang, J. Power Sources 185 (2008) 451–458.
[26] G. Zeng, Y. Tian, Y. Li, Int. J. Hydrogen Energy 35 (2010) 6726–6737.
[27] S. Hermann, R. Ecke, S. Schulz, T. Gessner, Microelectron. Eng. 85 (2008) 1979–1983.
[28] L.M. Aparicio, J. Catal. 165 (1997) 262–274.

[29] J. Yang, X. Wang, L. Li, K. X. Lu, W. Ding, Appl. Catal. B-Environ. 96 (2010) 232–237.
[30] H. Shimada, M. Imamura, N. Matsubayashi, T. Saito, T. Tanaka, T. Hayakawa, S. Kure, Top. Catal. 10 (2000) 265–271.
[31] X. Wang, N. Li, J.A. Webb, L.D. Pfefferle, G.L. Haller, Appl. Catal. B-Environ. 101 (2010) 21–30.
[32] A. Kuznetsova, I. Popova, J.T. Yates, M.J. Bronikowski, C.B. Huffman, J. Liu, R.E. Smalley, H.H. Hwu, J.G. Chen, J. Am. Chem. Soc. 123 (2001) 10699–10704.
[33] H. Shao, E.L. Kugler, D.B. Dadyburjor, S.A. Rykov, J.G. Chen, Appl. Catal. A-Gen. 356 (2009) 18–22.
[34] H.H. Hwu, B. Fruhberger, J.G. Chen, J. Catal. 221 (2004) 170–177.
[35] J.Z. Shyu, W.H. Weber, H.S. Gandhi, J. Phys. Chem. 92 (1988) 4964–4970.
[36] L.F. Liotta, A. Longo, G. Pantaleo, G. Di Carlo, A. Martorana, S. Cimino, G. Russo, G. Deganello, Appl. Catal. B-Environ. 90 (2009) 470–477.
[37] Y. Yang, S. Lim, G. Du, Y. Chen, D. Ciuparu, G.L. Haller, J. Phys. Chem. B 109 (2005) 13237–13246.
[38] G. Du, S. Lim, Y. Yang, C. Wang, L. Pfefferle, G.L. Haller, J. Catal. 249 (2007) 370–379.
[39] A.B. Hungría, N.D. Browining, R.P. Erni, M. Fernández-García, J.C. Conesa, J.A. Pérez-Omil, A. Martínez-Arias, J. Catal. 235 (2005) 251–261.
[40] S. Natesakhawat, R.B. Watson, X. Wang, U.S. Ozkan, J. Catal. 234 (2005) 496–508.